

8<sup>th</sup> International Conference on Photonic Technologies LANE 2014

## Improvement of the laser direct metal deposition process in 5-axis configuration

Didier Boisselier<sup>a,\*</sup>, Simon Sankaré<sup>a</sup>, Thierry Engel<sup>b</sup>

<sup>a</sup>: IREPA LASER, Pôle API, Parc d'Innovation, F-67400 ILLKIRCH, France

<sup>b</sup>: iCube – ipp – INSA Strasbourg, 24 blvd de la Victoire, 67084 Strasbourg

---

### Abstract

The implementation of the continuous 5-axis configuration can extend the limits of the Laser Direct Metal Deposition (LDMD) processes, especially when the complexity of the parts to be built is growing. In order to follow the profile of a part, we use the orientation of its growth axis. Although 5-axis machining is well known nowadays, LDMD processes require a specific optimization that depends on many parameters. Unlike conventional machining, it has to be noted that the speed variation tool tip affects the stability of deposition. Thus, we have to smooth trajectories in order to provide fluid movements and also to ensure the stability of deposition.

This article describes the method and results in the optimization of trajectories to build metallic parts with freeform. Optical sensors have been implemented in the focusing unit in order to follow the variations of the laser-powder-substrate interaction and also to detect the process instabilities. Thanks to the right use of a new and large 5 axis machine and specific setting trajectories, manufacturing parts in 5-axis, with no concession on the construction rate has been possible.

© 2014 Published by Elsevier B.V. This is an open access article under the CC BY-NC-ND license (<http://creativecommons.org/licenses/by-nc-nd/3.0/>).

Peer-review under responsibility of the Bayerisches Laserzentrum GmbH

**Keywords:** additive manufacturing; laser metal deposition; 5 axis manufacturing

---

---

\* Corresponding author. Tel.: +33-388655407 .  
E-mail address: [db@irepa-laser.com](mailto:db@irepa-laser.com)

## 1. Introduction

There is no need to demonstrate the advantages of the Additive Manufacturing Processes in industry any more. Among those, the Laser Direct Metal Deposition (LDMD) processes have shown very promising applications for the manufacturing of large parts [1], and parts repairing [2]. They are also good candidates for the processing of functionally graded materials parts [3-4].

These processes allow the manufacturing of parts directly from CAD files without any specific tool. In order to manufacture more complex parts however, a 5 axis configuration is necessary [5, 6, and 7].

Unlike machining, the process requires good stability of the operating conditions. Indeed, the parameters such as the laser power and the deposition velocity have a great influence on the geometry of the deposit [8, 9 and 10]. The main challenge is to keep the deposition velocity as constant as possible. But in the 5 axis configuration, several problems in relation with the tool velocity can be observed.

Singular points are one of those problems. Several authors mention that Computer Numerical Control (CNC) data can generate unexpected movements of the rotary axis. This phenomenon is due to the Inverse Kinematic Transformation, which generates singular positions during the calculation of the machine coordinates [11]. These singularities lead to large movements of the rotary axes through short displacements along the tool path. As a consequence, a significant drop in the tool velocity can be noted.

As illustrated in the drawing on fig.1, we can identify geometric errors as a source of instability. Indeed, the presence of chordal errors can lead to excessive variation of the tool orientation between two successive points of the trajectory.

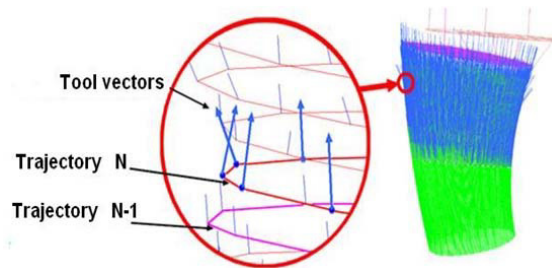


Fig. 1. Variation of the tool vector on a trajectory.

We can see many papers on the trajectory generation in multi-axis configuration, but, as far as we know, there is no report of a method that could optimize the construction rate for a 5-axis tool path.

In this work, we present a method that gain smooth trajectories with stable processing conditions. In this respect, the stability of the laser-material interaction has been checked using a commercial optical system for process monitoring. The relevance of this work has been shown by the manufacturing of specific parts for the aerospace industry.

## 2. Devices and methods

The laser deposition tests were carried out on a 5 axis LDMD machine specially designed by IREPA LASER (fig. 2 (a)).

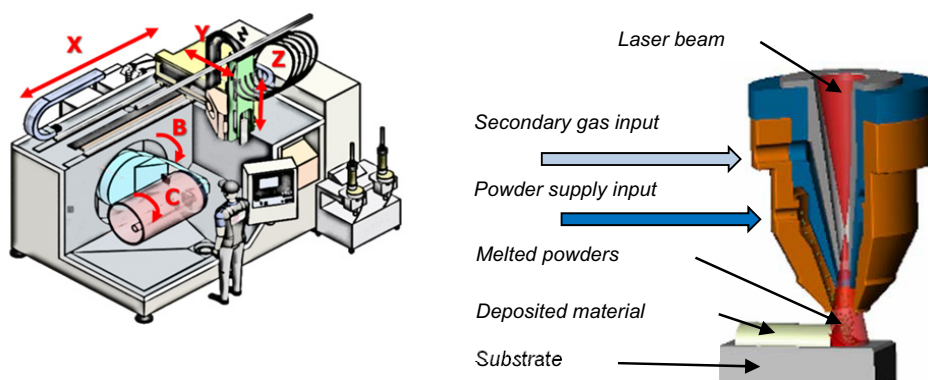


Fig. 2. (a) the 5 axis CNC workstation; (b) the coaxial laser cladding nozzle patented by IREPA LASER.

The deposition process is carried out using a coaxial nozzle patented by IREPA laser (fig. 2 (b)). This machine is equipped with a 6kW multimode fiber laser from IPG LASER. In this study only one module is used in order to work with a power lower than 380W.

The monitoring of the laser/material interaction is carried out with the Laser Welding Monitoring (LWM) system from the Precitec Company (Fig. 3). The system is based on three photodetectors, which are sensitive in different ranges of wavelength.

One of the sensors, called “P sensor”, is sensitive in the 400-600nm spectral interval. The second one, called “T sensor” is sensitive in the 1100-1800 nm wavelength range and the last one, named “R-sensor”, is sensitive in the 1060-1070 nm spectral range in order to detect the back reflected laser radiation from the process zone.

Another sensor “L-sensor” was used in order to monitor the incident laser power (the system was not calibrated and thus, only the variations of the laser power level could be tracked).

An acquisition module with LABVIEW software from National Instruments was used to collect these signals at a 5 kHz sample frequency and the collected data were analyzed with the Wavemetrics Igor Pro software.

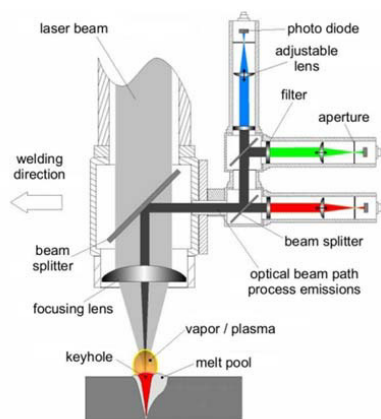


Fig. 3. The LWM system arrangement (Precitec courtesy).

Information of the axis movements is obtained directly from the monitoring functions of the CNC with a frequency of 166 Hz.

The geometric characterization of the deposits is made by using a focus variation microscope Infinitefocus from Alicona. This device provides the dimensions of the cord with a resolution of 4.2 microns in the XY plane and less than 1 micron in the Z direction.

All of the tests were performed with gas atomized AISI 316L powder (with 45-90 $\mu$ m grain size) clad on AISI 316L 3mm thickness plates.

Table. 1 Assignment of the process parameters.

P [W]	V [mm/s]	G [g/s]
250	33,3	0,11

### 3. Track thickness issues

As indicated previously, the operating parameters (Laser power (P), process velocity (V) and powder feed rate (G) – see table 1) affect the size of the cord including its thickness. Velocity fluctuations can therefore have a significant impact on the morphology of the deposit.

Indeed, a decrease of the process speed leads to a decrease of the deposited linear mass, which results in a slight oversize. Conversely, an increase of the process speed causes a hollow defect. If these variations are repeated during the part construction, significant instabilities appear (**Fehler! Verweisquelle konnte nicht gefunden werden.**).

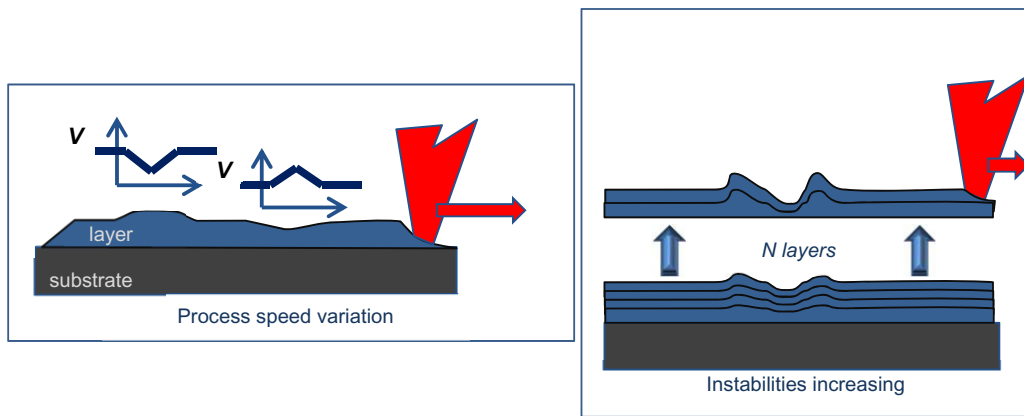


Fig. 4. Variation of the layer thickness with the process velocity variation.

However, the anticipation of variations in the thickness of track in relation with the process velocity is possible using a simple model.

Following the design of experiment and the substrate melting threshold defined by Jouvard et al. [13], it is possible to predict the deposit thickness.

Thus, three contributions are taken into account:

- Based on experimental results, a first relation gives the correspondence between the process parameters and the track thickness, as

$$\begin{cases} H_c = a_0 + a_1 \cdot P + a_2 \cdot V + a_3 \cdot P \cdot V \\ P \in [100; 250W] \\ V \in [8.3; 33.3 \text{ mm/s}] \end{cases} \quad \text{Eq.1}$$

Where  $H_c$  is the track thickness, the  $a_i$  coefficient are the effect of the factor,  $P$  is the laser power and  $V$  is the relative velocity between the LDMD nozzle and the part.

- Secondly, the synchronization between the tool point velocity and the laser power (implemented CNC function) is expressed in order to avoid the oversize defects when the velocity drops (track's end, cusp and inflection points...)

$$\begin{cases} P = C_{slope} \cdot V + P_{mini} \\ (P \in [P_{mini}; P_{program}]) \end{cases} \quad \text{Eq.2}$$

Where  $C_{slope}$  is the slope of the power/velocity law,  $P_{mini}$  is the laser power when the tool velocity is equal to zero and  $P_{program}$  is the laser power setting.

- At last, the power threshold defined by Jouvard et al. is used. This criterion allows the calculation of the minimal laser power in order to get the melting of the substrate. Here the energy brought by the melted powder is neglected.

$$P_{melt} = \frac{\sqrt{\pi k(T_{melt} - T_0)}}{2\beta\sqrt{\alpha\tau_{int}}} \quad \text{Eq.3}$$

Where  $k$  is the thermal conductivity of the substrate,  $T_{melt}$  and  $T_0$  are respectively the melting and the initial temperature of the substrate,  $\alpha$  is the thermal diffusivity,  $\tau_{int}$  is the interaction time between the laser beam and the substrate, and  $\beta$  is the ratio between the absorption coefficient and the interaction zone area.

Taking all these contributions into account, and based on the recording of a variation of velocity during a construction, it has been possible to evaluate its consequence on the track thickness (**Fehler! Verweisquelle konnte nicht gefunden werden.**).

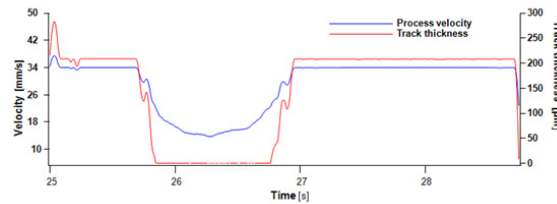


Fig. 5. Process velocity (blue curve) and corresponding track thickness.

These unwanted speed variations create defects on the parts. Some holes and surface roughness modifications can be observed (Fig. 6. Effect of speed variation on an aircraft part (courtesy of Dassault Aviation).

).

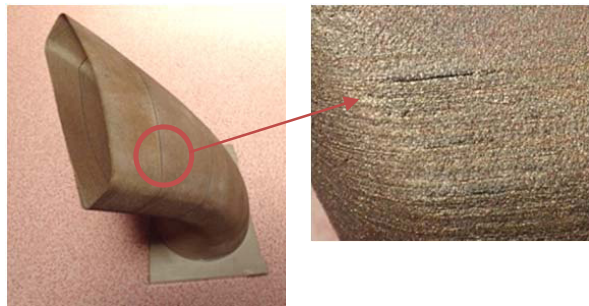


Fig. 6. Effect of speed variation on an aircraft part (courtesy of Dassault Aviation).

#### 4. Calculation of 5 axis tool path

The 5 axis trajectory is generated with a specific software developed in collaboration with DELCAM PLC. This software, named POWERCLAD®, enables the user to process a large diversity of parts with several manufacturing strategies.

The orientation between the nozzle and the workpiece is defined depending on the former tool path. The tool vector is thus calculated for each point of the trajectory (n) and oriented towards the previous layer (n-1) (Fig; 7).

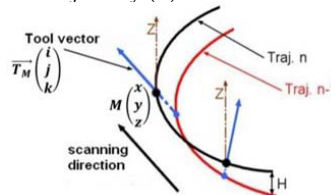


Fig. 7. Calculation of the tool vector using points on adjacent layers (n) and (n-1).

In this study, a circular path has been chosen. As a matter of fact, the tool moves along a circular curve, and each layer is shifted from one another, in order to create a 5 axis movement (Fig. 8).

This configuration was chosen in order to create singularities. Indeed, when the tool orientation approaches the vertical to the B&C rotating table (see Fig. 2), the probability to get a singularity increases: the B and C axis are subject to important variations.

In order to illustrate the benefit of smoothing, two trajectories were calculated: without smoothing (traj1) and with smoothing (traj2).

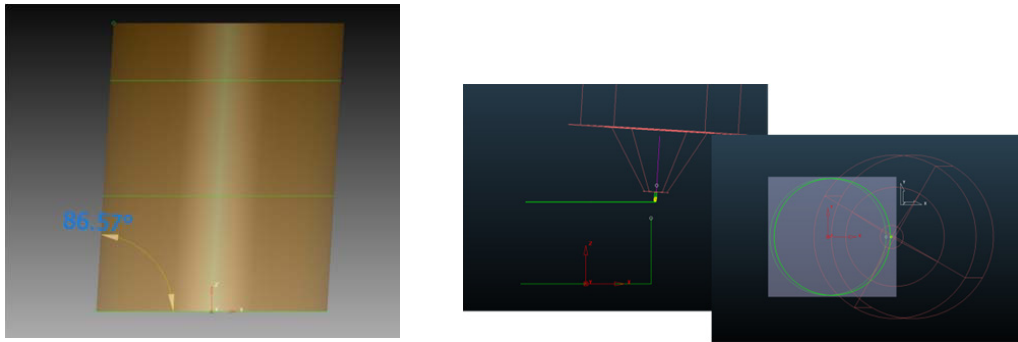


Fig. 8. (a) The tilted tube studied for trajectories generation; (b) The circular curve (in green) used to create the 5 axis tool path (on the left: a side view, on the right: view from above).

## 5. Calculation of 5 axis tool path

### 5.1. Influence of the smoothing on the trajectories

In fig. 9, we can see the original trajectory (traj1) that comprises two singularities along the tool path (**Fehler! Verweisquelle konnte nicht gefunden werden.**9). Close to the two given positions of the B axis, C axis encounters significant variations (about 160°) which is inhibiting the deposition rate, according to the P/V synchronization ( $V=0$ ,  $P=P_{min}=0$ ). As a result, a non-closed path is obtained. In these areas with low speed, no deposit occurs.

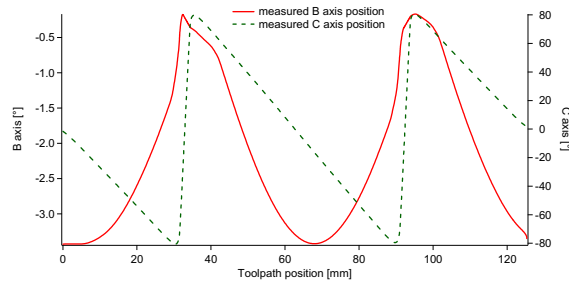


Fig. 9. Rotary axis positions along the original (non-smoothed) trajectory by default (traj1).

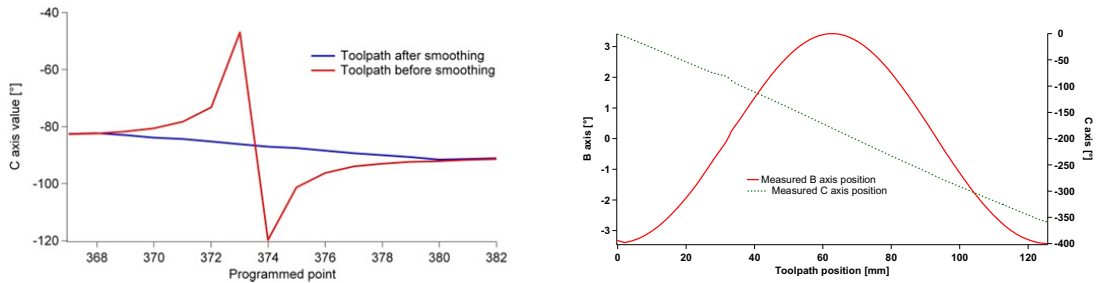


Fig. 10. (a) Linearization of the axis movements around the singularity; (b) The rotary axis position for the improved trajectory (traj2).

In a second test, two operations were performed:

- First we refined the discretization of the trajectory. This operation reduces the amplitude of the tool axis variation between two successive points of the trajectory.
- Then, the trajectory of the rotary axis was smoothed: the operator first sets the maximum curvature in relation with an acceptable variation of the rotary axis. The operator then sets the maximum variation of the rotary axis to be tolerated.

Once these operations are performed, the value of the tool axis is linearized around the singularity (Fig. 10 (a)).

Following these operations, the positions of the rotary axis show no more critical variations (Fig.10 (b)).

As a consequence, we get a significant improvement of the tool velocity variations. Only a few small defects are denoted and the deposit shows no critical anomaly any more (Fig. 11).

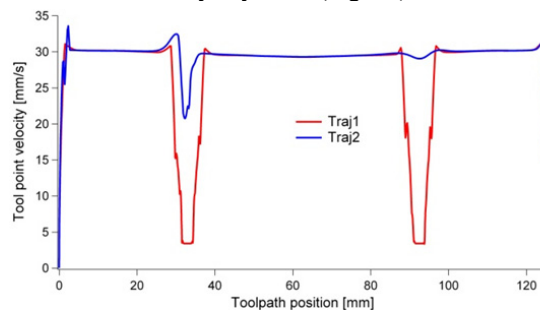


Fig. 11. Influence of smoothing the tool path on the trajectories. Original (traj 1) and modified (traj 2) (Programmed velocity 33,3 mm/s).

## 5.2. Use of the signals for process monitoring

These velocity variations and the corresponding laser-matter interaction modifications can be observed in a simple way thanks to the LWM photodetectors system. On a single track, when the velocity drops the power

decreases, the laser-matter interaction is lost, and all the signals (T,P,R,L) collapse (**Fehler! Verweisquelle konnte nicht gefunden werden.12**). At first glance, the different signals appear to follow the same trends and this can be easily verified using simple statistical tests

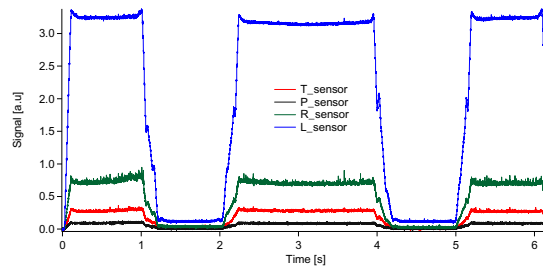


Fig. 12. Typical signals from the sensors during the deposition (traj1).

By calculating, the Bravais-Pearson product (moment of linear inter-correlation coefficient), we see that the signals are strongly correlated. This coefficient is given in **Fehler! Verweisquelle konnte nicht gefunden werden.**

$$BP_{coef} = \frac{\sigma_{xy}}{\sigma_x \sigma_y} \quad \text{Eq.4}$$

Where  $\sigma_{xy}$  is covariance between the random variables x and y,  $\sigma_x$  and  $\sigma_y$  are respectively the standard deviation of the variables x and y. In Table 2, showing the different BP products by pairs, we see that all the signals are quite well correlated.

Table 2. Bravais-Pearson linear inter-correlation coefficients of the signals.

Couple	BP coef
T/P	0.984
T/R	0.996
L/R	0.987
T/L	0.996

These results are in good agreement with the observations of Eriksson et al.[14]. However, in this study, the coefficients are closer to 1 still, especially for the T/P couple; this is because there is no plasma plume in the laser cladding process compared to laser welding.

In fig. 13, we show the typical signals got from the R and T sensors while machining the first 30mm track using the original traj. 1. We can notice that the standard deviation is a little less than 0.1 (0.1 to 1s range).

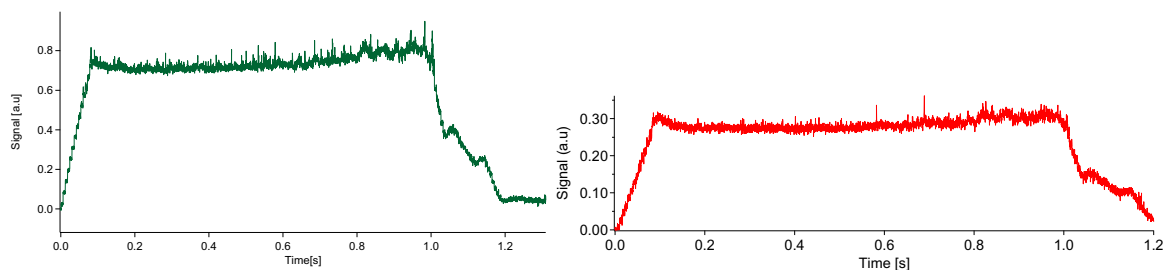


Fig. 13. (a) S from the R sensor during the first 30 mm of the track (traj1); (b) Signal from the T sensor during the first 30 mm of the track (traj1).



In order to see whether the signals T and R are correlated with an observable quantity in the parts or not, the thickness of the first 30 mm of the track was measured (Fig. 14).

The typical patterns are observed:

- the track begins with a small peak (0-1mm)
- there is a slight increase in the average value of the measurement over the length of the track (3-18mm).
- a drop of the deposit appears when the power falls down (position 20mm), due to a velocity drop (P/V synchronization)

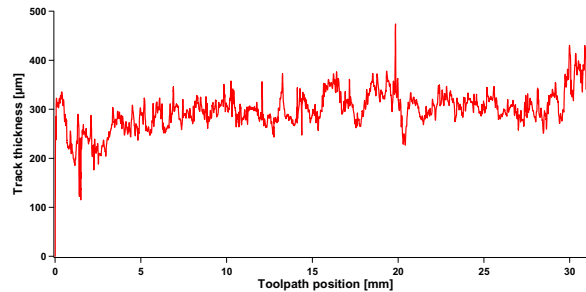


Fig. 14. Thickness of the first 30 mm of the track (traj1).

For the modified trajectory, the improvement of the tool path can be easily observed on the signals (Fig. 15). Small visible instabilities are seen when the velocity fluctuates (time 1.2s). The strong correlation between the signals remains and the average signal amplitude is the same as for the previous test.

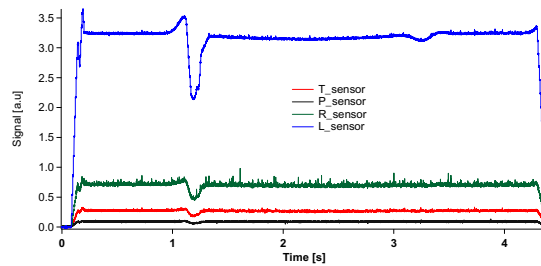


Fig. 15. Signals of the sensors during the deposition (traj2).

In order to illustrate the correlation between the signal and the track geometry (smoothed trajectory), the first second of the T signal is extracted (Fig. 16 (a)) and compared to the corresponding first 30 mm of the deposit thickness.

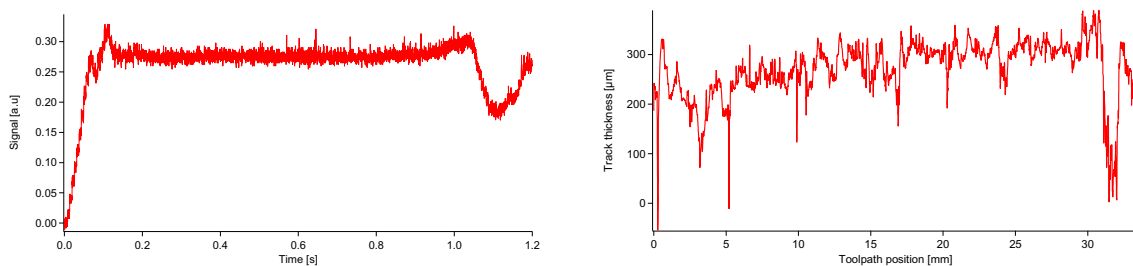


Fig. 16. (a) Signal from the T sensor during the first 30 mm of the track (traj2); (b) Thickness of the first 30 mm of the track (traj2).

The same patterns are observed:

- Small peaks appear at the beginning of the track
- The disturbance is preceded by a small peak (between 1 and 1.2s)

The noticeable variations of the T signal match with the variation of the tool path (Fig. 16 (b)). At 32 mm from the beginning of the track, a thickness reduction is noted on the track and the same variation is observed on the signals (time 1.05s). The variation of the laser power causes a decrease of the melted material which leads to a decrease of the signal.

### 5.3. Parts manufacturing

To validate the implemented solutions different parts were processed with the machine "MAGIC" (Fig. 17 (a)).



Fig. 17. (a) The machine MAGIC with its inert gas enclosure; (b) Samples manufactured in continuous 5 axis configuration.

Thanks to an appropriate choice of processing and smoothing parameters, it is now possible to manufacture mechanical parts with complex shapes (Fig. 17 (b)). These parts were built in continuous 5 axis configuration without process control.

## 6. Conclusion

Smoothing the trajectories of a 5-axis LDMD machine has been implemented in order to get fluid movements of the tool paths and also to reach stable velocities, even for complex shapes.

We use a commercial laser monitoring device in order to check the settings and also to detect the discrepancies of the process parameters. The geometry of the manufactured part is thus in good agreement with its CAD model. This work is a first step of the use of the LWM device for the monitoring of the CLAD® process. Further studies are in progress in order to correlate the signals with some detected process instabilities.

## Acknowledgments

The authors acknowledge the French government for supporting the FUI FALAFEL project N° F1004037Z.

## References

- [1] F.G. Arcella, D.H. Abbott et M.A. House, Titanium Alloy Structures for Airframe Application, by the Laser Forming Process, American Institute of Aeronautics and Astronautics, 1465, (2000).
- [2] D. Gill, J. Smugeresky, C. Atwood, Laser Engineered Net Shaping (LENS®) for the Repair and Modification of NWC Metal Components, SANDIA report 2006, available at <http://prod.sandia.gov/techlib/access-control.cgi/2006/066551.pdf> (june 2013)
- [3] K.Shin , H.Natu , D.Dutta , J.Mazumder, A method for the design and fabrication of heterogeneous objects, Materials and Design,24, (2003), p 339-353.
- [4] M.S. Domack, J.M. Baughman, Development of nickel-titanium graded composition components" Rapid

Prototyping Journal, 11, 1, (2005), pp.41 – 51.

[5] J.O Milewski, G.K Lewis, D.J Thoma, G.I Keel, R.B Nemec, R.A Reinert, Directed light fabrication of a solid metal hemisphere using 5-axis powder deposition, Journal of Materials Processing Technology, 75, 1–3, (1998), pp. 165–172.

[6] M. Kerschbaumer, G. Ernst, P. O’Leary, Tool Path Generation for 5-Axis Laser cladding, Proc. 4th International Conference on Laser Assisted Net Shape Engineering (LANE), Erlangen (Germany), 21.-24.Sep. 2004

[7] R. Dwivedi, R. Kovacevic, An expert system for generation of machine inputs for laser-based multi-directional metal deposition, International Journal of Machine Tools and Manufacture, 46, 14, (2006), pp. 1811–1822.

[8] U. de Oliveira, V. Ocelik, J.Th.M. De Hosson, Analysis of coaxial laser cladding processing conditions, Surface & Coatings Technology, 197, (2005), pp. 127–136.

[9] S.Sankaré, Development of a rapid manufacturing process of mechanical components in titanium alloys by laser micro-cladding, PhD thesis, 10/2007, University of Strasbourg, (In french).

[10] H.El Cheikh, B.Courant, S.Branchu, Xiaowei Huang, Jean-Yves Hascoët, R.Guillén, Direct Laser Fabrication process with coaxial powder projection of 316L steel. Geometrical characteristics and microstructure characterization of wall structures, Optics and Lasers in Engineering, 50, 12, (2012), pp. 1779–1784.

[11] B.S. So, D.H. Park, Y. Cho, T.J. Kim, T.S. Song, T.J. Ko, An analytic model for tool trajectory error in 5-axis machining, Journal of Achievements in Materials and Manufacturing Engineering, 31, 2, (2008), pp.570-575.

[12] O.Fréneaux, J.B. Poulet, O.Lépré, G.Montavon: Coaxial nozzle for surface treatment by laser irradiation with supply of materials in powder form, EUR patent n° 0574580, US patent n° 5418350.

[12] J.M.Jouvard, D. Grevey, F. Lemoine, A. Vannes, Dépôts par projection de poudres dans un faisceau laser Nd : YAG : cas des faibles puissances, J. de Physique III, 1997, pp. 2265-2274.

[14] I.Eriksson, J.Powell, A.F.H. Kaplan, Signal overlap in the monitoring of laser welding, Measurement Science and Technology, 21, (2010).